

Market calibration under a long memory stochastic volatility model

Jan Pospíšil & Tomáš Sobotka

To cite this article: Jan Pospíšil & Tomáš Sobotka (2017): Market calibration under a long memory stochastic volatility model, Applied Mathematical Finance, DOI: [10.1080/1350486X.2017.1279977](https://doi.org/10.1080/1350486X.2017.1279977)

To link to this article: <http://dx.doi.org/10.1080/1350486X.2017.1279977>



Published online: 25 Jan 2017.



Submit your article to this journal [↗](#)



View related articles [↗](#)



View Crossmark data [↗](#)

Market calibration under a long memory stochastic volatility model

Jan Pospíšil and Tomáš Sobotka

New Technologies for the Information Society, European Centre of Excellence, University of West Bohemia, Plzeň, Czech Republic

ABSTRACT

In this article, we study a long memory stochastic volatility model (LSV), under which stock prices follow a jump-diffusion stochastic process and its stochastic volatility is driven by a continuous-time fractional process that attains a long memory. LSV model should take into account most of the observed market aspects and unlike many other approaches, the volatility clustering phenomenon is captured explicitly by the long memory parameter. Moreover, this property has been reported in realized volatility time-series across different asset classes and time periods. In the first part of the article, we derive an alternative formula for pricing European securities. The formula enables us to effectively price European options and to calibrate the model to a given option market. In the second part of the article, we provide an empirical review of the model calibration. For this purpose, a set of traded FTSE 100 index call options is used and the long memory volatility model is compared to a popular pricing approach – the Heston model. To test stability of calibrated parameters and to verify calibration results from previous data set, we utilize multiple data sets from NYSE option market on Apple Inc. stock.

ARTICLE HISTORY

Received 8 January 2015
Accepted 15 December 2016

KEYWORDS

European call option;
stochastic volatility; long
memory; fractional process;
market calibration

1. Introduction

The purpose of this article is to revisit a jump-diffusion and fractional stochastic volatility approach proposed by Intarasit and Sattayatham (2011). Using our alternative formula for pricing European options, we present empirical calibration results and we comment on suitability of this approach.

First of all, we define a long-range dependence (LRD or equivalently a long memory) property. Let (Ω, \mathcal{F}, P) be a generic probability space that is used for all stochastic processes in this article unless explicitly stated otherwise. Let $(X_t)_{t \in \mathbb{R}^+}$ be a stationary stochastic process defined on the probability space. Then, its auto-covariance function for arbitrary real $s, t : 0 \leq s < t$ depends only on the lag $k := t - s$ and is denoted by $\gamma_X(k)$,

$$\gamma_X(k) = E[(X_s - EX_s)(X_{s+k} - EX_{s+k})].$$

A stochastic process X_t is said to have a LRD if

$$\lim_{k \rightarrow +\infty} \frac{\gamma_X(k)}{Ck^{-\alpha}} = 1, \quad (1)$$

where both C and α are constants and $\alpha \in (0, 1)$. Also, the sum of auto-covariances for different lags diverges,

$$\sum_{k=1}^{+\infty} \gamma_X(k) = +\infty. \quad (2)$$

One can understand the LRD phenomenon quite intuitively. For increasing lag, the dependence might be small, but its cumulative effect is not negligible (due to (2)).

One of the first evidences of LRD in market volatility comes from Taylor (1986) and Ding, Granger and Engle (1993). In both studies, a strong evidence of autocorrelation of absolute returns is presented (even for longer lags). Authors also noticed that correlation estimates decay significantly slower for absolute returns than for the returns themselves. Breidt, Crato and De Lima (1998) used spectral tests and R/S analysis to estimate a long memory parameter for volatility of market indexes' daily returns from 1962 to 1989. To incorporate the long memory phenomenon into volatility modelling, Bollerslev and Mikkelsen (1996) suggested a modification of a well-known GARCH (Generalized Auto-Regressive Conditional Heteroskedasticity) model – fractionally integrated GARCH. The authors compare several models in terms of forecasting realized volatility and they also compare model prices of (synthetic) options. Further improvement of the ARCH-type approach to option pricing is suggested by Zumbach and Fern'Andez (2013) and Zumbach and Fern'Andez (2014). They provide an insight into construction of the risk-neutral measure and explain how to estimate the parameters, reproduce the volatility smile and the term structure of the surfaces without any calibration of the observed option prices.

Another discrete-time modelling approach that captures LRD is ARFIMA model (fractionally integrated ARMA) (Granger and Joyeux 1980). Martens, Van Dijk and De Pooter (2004) have shown, using their own study alongside similar works by various authors, that ARFIMA models can provide more satisfactory results than GARCH-type approaches. The estimates of a fractional differencing parameter for market volatility typically lie in $[0.2, 0.4]$ which is equivalent to the Hurst exponent ranging in $[0.7, 0.9]$. Koopman, Jungbacker and Hol (2005) also empirically confirmed that long memory ARFIMA models seem to provide the most accurate forecasts of realized volatility. Lately, Asai, McAleer and Medeiros (2012) introduced a new correction term for the ARFIMA model with respect to volatility modelling. For an empirical comparison of ARMA and ARFIMA models, see e.g. the thesis by Čekal (2012). Beran et al. (2013), Zumbach (2013) and the references therein provide a comprehensive review of recent advances in discrete-time long memory modelling.

Many practitioners prefer continuous-time models for calibration to the whole volatility surface. Pioneering a long memory stochastic volatility (LSV), Comte and Renault (1998) introduced a modification of the Hull–White model. The stochastic

volatility process is driven by a fractional Brownian motion (fBm), i.e. a centred Gaussian process, $(B_t)_{t \in \mathbb{R}^+}$, defined via its covariance structure

$$E[B_t B_s] = \frac{1}{2} (t^{2H} + s^{2H} - |t - s|^{2H}), \quad (3)$$

where H is a constant in $(0,1)$, commonly known as the Hurst exponent. This process possesses many interesting properties, most noticeably, for $H \in (1/2, 1)$, fBm exhibits a LRD (Mandelbrot and Van Ness 1968). Comte and Renault also comment on a no-arbitrage condition which is satisfied by a market model with the suggested dynamics alongside a standard class of admissible portfolios. This differs from a situation where market dynamics is due to the fractional Black–Scholes model (i.e. stock prices follow a geometric fBm). In that case, one has to come up with a different integration theory accompanied by a different class of admissible strategies (on that matter, see e.g. Øksendal 2003). Comte, Coutin and Renault (2012) introduced a more refined model with more degrees of freedom where stochastic volatility follows a fractional CIR process. Since fBm is not a semimartingale for $H \neq 0.5$, we cannot use a well-developed Itô stochastic calculus on any of the aforementioned fractional stochastic volatility models.

Intarasit and Sattayatham (2011) came up with a new LSV model which would be subject to the main focus of this article. Authors applied theoretical results by Thao (2006) and Zähle (1998) to overcome restrictions inherited from the usage of fBm. They started with fBm in the Liouville form (Mandelbrot and Van Ness 1968),

$$B_t = \frac{1}{\Gamma(H + 1/2)} \left[Z_t + \int_0^t (t - s)^{H-1/2} dW_s \right],$$

where $Z_t = \int_{-\infty}^0 [(t - s)^{H-1/2} - (-s)^{H-1/2}] dW_s$ and $(W_t)_{t \in \mathbb{R}^+}$ is a standard Wiener

process. The stochastic process Z_t has continuous trajectories and thus, for the sake of long memory, one can consider only the following part of B_t with the Hurst exponent $H \in (1/2, 1)$.

$$\hat{B}_t = \int_0^t (t - s)^{H-1/2} dW_s. \quad (4)$$

Thao (2006) showed that one can approximate \hat{B}_t by

$$\hat{B}_t^\varepsilon = \int_0^t (t - s + \varepsilon)^{H-1/2} dW_s; \quad \hat{B}_t^\varepsilon \xrightarrow{L^2(\Omega)} \hat{B}_t, \quad (5)$$

as $\varepsilon \rightarrow 0^+$. Also, \hat{B}_t^ε is a semimartingale with respect to the filtration $(\mathcal{F}_t)_{t \in \mathbb{R}^+}$ generated by the standard Wiener process W_t . Intarasit and Sattayatham (2011) proposed a jump-diffusion model with approximative fractional volatility. In this paper, we focus on similar dynamics of the stock prices that follow a system of two stochastic

differential equations which under a risk-neutral probability measure¹ take the following form,

$$dS_t = rS_t dt + \sqrt{v_t}S_t dW_t^{(1)} + Y_t S_{t-} dN_t, \quad (6)$$

$$dv_t = -\kappa(v_t - \bar{v})dt + \xi\sqrt{v_t} d\hat{B}_t^\varepsilon, \quad (7)$$

where κ, \bar{v}, ξ are model parameters such that, κ is a mean-reversion rate, \bar{v} stands for an average volatility level and, finally, ξ is so-called volatility of volatility. Under the notation S_{t-} , we understand $\lim_{\tau \rightarrow t-} S_\tau$ and $(N_t)_{t \in \mathbb{R}^+}$, $(W_t^{(1)})_{t \in \mathbb{R}^+}$ are a Poisson process and a standard Wiener process, respectively. Y_t denotes an amplitude of a jump at t (conditional on occurrence of the jump) and differential $d\hat{B}_t^\varepsilon$ corresponds to the following integral which Thao and Nguyen (2003) defined for arbitrary stochastic process with bounded variation $(F_t)_{t \in \mathbb{R}^+}$,

$$I_t = \int_0^t F_s d\hat{B}_s^\varepsilon := F_t \hat{B}_t^\varepsilon - \int_0^t \hat{B}_s^\varepsilon dF_s - [F, \hat{B}^\varepsilon]_t, \quad (8)$$

provided the right-hand side integral exists in a Riemann–Stieltjes sense, while $[F, \hat{B}^\varepsilon]_t$ being a mixed variation of F_t and \hat{B}_t^ε .

The use of approximation \hat{B}_t^ε instead of fBm provides several advantages. Most significantly, we are able to derive a pricing PDE using Itô calculus and standard hedging arguments. Moreover, using theoretical results of Thao and Nguyen (2003), we can transform volatility process into standard settings similarly as was shown by Intarasit and Sattayatham (2011),

$$dv_t = (a\xi\varphi_t\sqrt{v_t} - \theta + \kappa v_t)dt + \xi\varepsilon^a\sqrt{v_t} dW_t^{(2)}, \quad (9)$$

where $a := H - 1/2$, $\theta := \kappa\bar{v}$ is a constant and φ_t represents an Itô integral,

$$\varphi_t = \int_0^t (t - s + \varepsilon)^{H-3/2} dW_s^{(3)}, \quad (10)$$

$(W_t^{(2)})_{t \in \mathbb{R}^+}$, $(W_t^{(3)})_{t \in \mathbb{R}^+}$ are standard Wiener processes. To have a more realistic model of market dynamics, we also add an instantaneous correlation $\rho: \mathbb{E}[W_t^{(1)}W_t^{(2)}] = \rho$ to mimic the stock-volatility leverage effect. Also, we assume $W_t^{(3)}$ is stochastically independent on $W_t^{(1)}$, $W_t^{(2)}$ and the jump part $Y_t S_{t-} dN_t$ which is yet to be defined.

2. An alternative semi-closed form solution

Up to now, we have introduced a theoretical background for the model mainly using the original research by Intarasit and Sattayatham (2011). In this section, we consider a model with dynamics (6) and (7) and we derive an alternative formula for pricing

European contracts and thereafter, we show, employing empirical data sets, that this formula can be efficiently used for applications in practise, such as a market calibration.

We utilize dynamics (6) and (7) with process N_t defined as

$$N_t = \sum_{i=1}^{P_t} Y_i, \quad (11)$$

where (Y_n) are *i.i.d.* random variables $Y_n = \exp\{\alpha_j + \gamma_j \psi_n\} - 1$, $\psi_n \sim \mathcal{N}(0, 1)$ and P_t is a Poisson process with hazard rate λ .

Unlike in case of Intarasit and Sattayatham (2011), we will assume² that the jump part is stochastically independent on diffusion processes in market dynamics (6) and (7) which will significantly simplify the option pricing problem. Instead of solving partial integral differential equations with respect to (6) and (7), we consider the following system of market dynamics without jumps.

$$dS_t = rS_t dt + \sqrt{v_t} S_t dW_t^{(1)}, \quad (12)$$

$$dv_t = \alpha dt + \beta \sqrt{v_t} dW_t^{(2)}, \quad (13)$$

where the functions α and β take the following form $\alpha = \alpha(S_t, v_t, t) := (a\xi\varphi_t - \kappa)v_t + \theta$, $\beta = \beta(S_t, v_t, t) := \xi\varepsilon^a$. We will derive the valuation PDE which can be solved using the Fourier method. The price of a European option is expressed in terms of characteristic functions and to include jumps in the stock price process, it is sufficient to multiply these characteristic functions with their jump counterparts.³ A fair price of a vanilla option V is expressed as a discounted expectation of the terminal payoff. In case of a call option, this reads

$$\begin{aligned} V_c(S_t, v_t, t) &= e^{-r\tau} \mathbb{E}[(S_T - K)^+] \\ &= S_t P_1(x_t, v_t, \tau) - e^{-r\tau} K P_2(x_t, v_t, \tau) \\ &= e^{x_t} P_1(x_t, v_t, \tau) - e^{-r\tau} K P_2(x_t, v_t, \tau), \end{aligned} \quad (14)$$

where parameters of the contract K and $\tau := T - t$ represent a strike price and time to maturity, respectively. P_1, P_2 can be interpreted as the risk-neutral probabilities that option expires in the money conditional on the value of $x_t = \ln S_t$ and finally, r is assumed to be a uniquely determined risk-free rate constant.

Applying standard hedging arguments alongside constant risk-free rate paradigm, one arrives at the initial value problem (Sobotka 2014),

$$-\frac{\partial V_c}{\partial \tau} + \frac{1}{2} v_t \frac{\partial^2 V_c}{\partial x_t^2} + \left(r - \frac{1}{2} v_t\right) \frac{\partial V_c}{\partial x_t} + \rho \beta v_t \frac{\partial^2 V_c}{\partial v_t \partial x_t} - r V_c + \frac{1}{2} v_t \beta^2 \frac{\partial^2 V_c}{\partial v_t^2} + \alpha \frac{\partial V_c}{\partial v_t} = 0; \quad (15)$$

$$V_c(S_T, v_T, \tau = 0) = (S_T - K)^+. \quad (16)$$

As we would like to express probabilities P_1, P_2 , we input (14) therein. Equation (15) has to be satisfied for any combination of parameters $K, r \in \mathbb{R}, \tau \in \mathbb{R}^+$ and for

any price $S_t \geq 0$. Thus, we are able to set $K = 0$, $S_t = 1$, to obtain a PDE with respect to P_1 only.

$$-\frac{\partial P_1}{\partial \tau} + \frac{1}{2}v_t \frac{\partial^2 P_1}{\partial x_t^2} + \left(r + \frac{1}{2}v_t\right) \frac{\partial P_1}{\partial x_t} + \rho\beta v_t \frac{\partial^2 P_1}{\partial v_t \partial x_t} + \frac{1}{2}v_t \beta^2 \frac{\partial^2 P_1}{\partial v_t^2} + (\alpha + \rho\beta v_t) \frac{\partial P_1}{\partial v_t} = 0. \quad (17)$$

Following similar arguments, we retrieve a PDE for P_2 only by setting $S_t = 0$, $K = -1$.

$$-\frac{\partial P_2}{\partial \tau} + \frac{1}{2}v_t \frac{\partial^2 P_2}{\partial x_t^2} + \left(r - \frac{1}{2}v_t\right) \frac{\partial P_2}{\partial x_t} + \rho\beta v_t \frac{\partial^2 P_2}{\partial v_t \partial x_t} + \frac{1}{2}v_t \beta^2 \frac{\partial^2 P_2}{\partial v_t^2} + \alpha \frac{\partial P_2}{\partial v_t} = 0. \quad (18)$$

Instead of solving the system of two PDEs (17) and (18) directly, we express characteristic functions $f_j = f_j(\phi, \tau)$, $j = 1, 2$. After analytical expressions for f_j are known, we can easily obtain P_j using the inverse Fourier transform,

$$P_j = \frac{1}{2} + \frac{1}{\pi} \int_0^\infty \Re \left[\frac{e^{i\phi \ln(K) f_j}}{i\phi} \right] d\phi, \quad (19)$$

where $\Re(x)$ denotes a real part of a complex number x . As in the original paper by Heston (1993), we are looking for characteristic functions f_j in the form,

$$f_j = \exp\{C_j(\tau, \phi) + D_j(\tau, \phi)v_t + i\phi x\}. \quad (20)$$

As a direct consequence of the discounted version of Feynman–Kac theorem (as e.g. in Shreve 2004), f_j follows PDE (17) and (18). First, we substitute assumed expression (20) with respect to f_1 .

$$\begin{aligned} & -\left(\frac{\partial C_1}{\partial \tau} + v_t \frac{\partial D_1}{\partial \tau}\right) f_1 + \rho\beta v_t i\phi D_1 f_1 - \frac{1}{2}v_t \phi^2 f_1 + \frac{1}{2}v_t \beta^2 D_1^2 f_1 \\ & + \left(r + \frac{1}{2}v_t\right) i\phi f_1 + (\alpha + \rho\beta v_t) f_1 D_1 = 0, \end{aligned} \quad (21)$$

f_1 cannot be identically equal to zero which enables us to get the following relation.

$$\begin{aligned} & -\frac{\partial C_1}{\partial \tau} + v_t \frac{\partial D_1}{\partial \tau} + \rho\beta v_t i\phi D_1 - \frac{1}{2}v_t \phi^2 + \frac{1}{2}v_t \beta^2 D_1^2 \\ & + \left(r + \frac{1}{2}v_t\right) i\phi + (\alpha + \rho\beta v_t) D_1 = 0. \end{aligned} \quad (22)$$

Now, we are ready to substitute back for α . After rearranging terms with C_1, D_1 and factoring out v_t , we obtain the upcoming PDE,

$$v_t \left[-\frac{\partial D_1}{\partial \tau} + \rho\beta i\phi D_1 - \frac{1}{2}\phi^2 + \frac{1}{2}\beta^2 D_1^2 + \frac{1}{2}i\phi + (a\xi\varphi_0 - \kappa + \rho\beta) D_1 \right] - \frac{\partial C_1}{\partial \tau} + ri\phi + \theta D_1 = 0, \quad (23)$$

where we recall that φ_t is a martingale and $\varphi_0 = E[\varphi_t]$ is used. None of the terms outside brackets involves v_t ; hence, we can split (23) into a system of two equations.

$$\frac{\partial D_1}{\partial \tau} = \rho\beta i\phi D_1 - \frac{1}{2}\phi^2 + \frac{1}{2}\beta^2 D_1^2 + \frac{1}{2}i\phi + (a\xi\varphi_0 - \kappa + \rho\beta) D_1; \quad (24)$$

$$\frac{\partial C_1}{\partial \tau} = ri\phi + \theta D_1, \quad (25)$$

provided $v_t > 0$ for $t : 0 \leq t \leq T$. Following the same steps, one can obtain a similar system for f_2 as well. As a result thereof, characteristic functions f_j defined by (20) have to satisfy the following system of four differential equations

$$\frac{\partial D_1}{\partial \tau} = \rho\beta i\phi D_1 - \frac{1}{2}\phi^2 + \frac{1}{2}\beta^2 D_1^2 + \frac{1}{2}i\phi + (a\xi\varphi_0 - \kappa + \rho\beta)D_1; \quad (26)$$

$$\frac{\partial D_2}{\partial \tau} = \rho\beta i\phi D_2 - \frac{1}{2}\phi^2 + \frac{1}{2}\beta^2 D_2^2 - \frac{1}{2}i\phi + (a\xi\varphi_0 - \kappa)D_2; \quad (27)$$

$$\frac{\partial C_j}{\partial \tau} = ri\phi + \theta D_j; \quad (28)$$

with respect to the initial condition

$$C_j(0, \phi) = D_j(0, \phi) = 0, \quad (29)$$

where $j = 1, 2$. The first two equations for D_j are known as the Riccati equations with constant coefficients. Once D_j are obtained, one can solve the last two ODE's by a direct integration.

First, we show how to express D_j from the Riccati equations. For the sake of a simpler notation, we will rewrite Equations (26) and (27) using abbreviated form.

$$\frac{\partial D_j(\tau, \phi)}{\partial \tau} = A_j D_j^2 + B_j D_j + K_j, \quad (30)$$

where A_j, B_j and $K_j \in \mathbb{C}$. Let us also denote:

$$\Delta_j = \sqrt{B_j^2 - 4A_j K_j}; \quad Y_j = \frac{-B_j + \Delta_j}{2A_j}; \quad g_j = \frac{B_j - \Delta_j}{B_j + \Delta_j}.$$

Proposition 2.1: Assuming $A_j \neq 0$ for $j = 1, 2$, Riccati equation (30) attain an analytical solution with respect to the initial condition $D_j(0, \phi) = 0$,

$$D_j(\tau, \phi) = \frac{Y_j(1 - e^{\Delta_j \tau})}{1 - g_j e^{\Delta_j \tau}}.$$

Proof: Without loss of generality, we will solve the equation for a fixed index j and for $y := D_j$, while $A := A_j, B := B_j, K := K_j$

$$y' = Ay^2 + By + K, \quad (31)$$

$$Ay' = (Ay)^2 + ABY + AK, \quad (32)$$

Since A, B and K are constant in time (or with respect to τ), we are able to substitute $v = Ay$; $v' = Ay' + A'y = Ay'$.

$$v' = v^2 + Bv + AK, \quad (33)$$

$$-\frac{u''}{u} = -B\frac{u'}{u} + AK, \quad (34)$$

where $v = -u'/u$; $v' = -[u''u - (u')^2]/u^2 = v^2 - u''/u'$. The equation can be rewritten in the following form

$$0 = u'' - Bu' + AKu. \quad (35)$$

We are able to solve (35) explicitly.

$$\begin{aligned} u(\tau) &= I_1 \exp\left\{\frac{B - \sqrt{B^2 - 4AK}}{2}\tau\right\} + I_2 \exp\left\{\frac{B + \sqrt{B^2 - 4AK}}{2}\tau\right\} \\ &= I_1 e^{((B-\Delta)/2)\tau} + I_2 e^{((B+\Delta)/2)\tau}, \end{aligned}$$

where $I_1, I_2 \in \mathbb{R}$ are both constants can be expressed due to the initial condition:

$$\begin{aligned} u'(0) &= I_1 \left(\frac{B-\Delta}{2}\right) + I_2 \left(\frac{B+\Delta}{2}\right) = 0, \\ u(0) &= I_1 + I_2 = \gamma; \gamma \in \mathbb{R} - \{0\}. \end{aligned}$$

Solving the system of two linear equations, we retrieve I_1, I_2 ,

$$I_1 = \gamma \frac{B+\Delta}{2\Delta},$$

$$I_2 = -\gamma \frac{B-\Delta}{2\Delta},$$

and the solution $u(\tau)$,

$$u(\tau) = \gamma \left[\left(\frac{B+\Delta}{2\Delta}\right) e^{((B-\Delta)/2)\tau} - \left(\frac{B-\Delta}{2\Delta}\right) e^{((B+\Delta)/2)\tau} \right]. \quad (36)$$

To obtain $y(\tau)$, we go through steps (31)–(35) backwards. The first derivative of u takes the form

$$u' = \gamma \left[\frac{AK}{\Delta} e^{((B-\Delta)/2)\tau} - \frac{AK}{\Delta} e^{((B+\Delta)/2)\tau} \right] \quad (37)$$

and since $v = -u'/u$, v reads

$$v = \frac{-2AK(e^{((B-\Delta)/2)\tau} - e^{((B+\Delta)/2)\tau})}{(B+\Delta)e^{((B-\Delta)/2)\tau} - (B-\Delta)e^{((B+\Delta)/2)\tau}}.$$

Using $y = v/A$, one can obtain the solution,

$$\begin{aligned} y &= \frac{-2K(e^{((B-\Delta)/2)\tau} - e^{((B+\Delta)/2)\tau})}{(B+\Delta)e^{((B-\Delta)/2)\tau} - (B-\Delta)e^{((B+\Delta)/2)\tau}} \\ &= \frac{-2K(e^{((B-\Delta)/2)\tau} - e^{((B+\Delta)/2)\tau})}{(B+\Delta)e^{((B-\Delta)/2)\tau}(1 - (B-\Delta)/(B+\Delta)e^{\Delta\tau})} \\ &= \frac{-2K/(B+\Delta)(1 - e^{\Delta\tau})}{1 - (B-\Delta)/(B+\Delta)e^{\Delta\tau}}. \end{aligned} \quad (38)$$

Hence, we have arrived at the expression in Proposition 2.1.

In the next step, we integrate the right-hand side of (28) for $t \in [0, \tau]$ to express C_j .

$$\begin{aligned}
 C_j(\tau, \phi) &= r\phi\tau + \theta \int_0^\tau D_j(t, \phi) dt \\
 &= r\phi\tau + \theta \int_0^\tau \frac{Y_j(1 - e^{\Delta_j t})}{1 - g_j e^{\Delta_j t}} dt \\
 &= r\phi\tau + \theta Y_j \left[\tau + \int_0^\tau \frac{(g_j - 1)e^{\Delta_j t}}{1 - g_j e^{\Delta_j t}} dt \right] \\
 &= r\phi\tau + \theta Y_j \tau - \theta Y_j \frac{g_j - 1}{\Delta_j g_j} \ln \left(\frac{1 - g_j e^{\Delta_j \tau}}{1 - g_j} \right) \\
 &= r\phi\tau + \theta Y_j \tau - \frac{\theta}{A} \ln \left(\frac{1 - g_j e^{\Delta_j \tau}}{1 - g_j} \right).
 \end{aligned} \tag{39}$$

Characteristic functions f_j , under the original notation, take the following form

$$f_j(\tau, \phi) = \exp \left\{ C_j(\tau, \phi) + D_j(\tau, \phi)v_t + i\phi \ln(S_t) + \psi_j(\phi)\tau \right\},$$

with

$$\begin{aligned}
 C_j(\tau, \phi) &= r\phi i\tau + \theta Y_j \tau - \frac{2\theta}{\beta^2} \ln \left(\frac{1 - g_j e^{d_j \tau}}{1 - g_j} \right), \\
 D_j(\tau, \phi) &= Y_j \left(\frac{1 - e^{d_j \tau}}{1 - g_j e^{d_j \tau}} \right), \\
 \psi_2(\phi) &= -\lambda_j i\phi \left(e^{\alpha_j + (\gamma_j^2/2)} - 1 \right) + \lambda_j \left(e^{i\phi\alpha_j - (\phi^2\gamma_j^2/2)} - 1 \right), \\
 \psi_1(\phi) &= \psi_2(\phi - i), \\
 Y_j &= \frac{b_j - \rho\beta\phi i + d_j}{\beta^2}, \\
 g_j &= \frac{b_j - \rho\beta\phi i + d_j}{b_j - \rho\beta\phi i - d_j}, \\
 d_j &= \sqrt{(\rho\beta\phi i - b_j)^2 - \beta^2(2u_j\phi i - \phi^2)}, \\
 \beta &= \xi\varepsilon^{H-1/2}, \\
 u_1 &= 1/2, \quad u_2 = -1/2, \quad \theta = \kappa\bar{v}, \quad b_1 = \kappa - (H - 1/2)\xi\varphi_0 - \rho\beta, \\
 b_2 &= \kappa - (H - 1/2)\xi\varphi_0.
 \end{aligned}$$

To obtain the price of a European call, one numerically computes the integral in Equation (19). The result thereof goes into the first part of the formula, expression (14).

Table 1. Price differences for various choices of the upper integration limit in integral (19) across various parameter sets.^a

Upper integration limit	50	100	150	200	250	300
ITM Average absolute differences	2.1×10^{-8}	2.8×10^{-8}	2.4×10^{-8}	2.5×10^{-8}	2.1×10^{-8}	2.1×10^{-8}
ITM 99-percentile differences	1.5×10^{-7}	1.6×10^{-7}	1.4×10^{-7}	1.4×10^{-7}	1.4×10^{-7}	1.4×10^{-7}
ITM Maximal absolute differences	1.1×10^{-3}	1.1×10^{-3}	1.1×10^{-3}	1.1×10^{-3}	1.1×10^{-3}	1.1×10^{-3}
ATM Average absolute differences	2.6×10^{-8}	3.3×10^{-8}	2.7×10^{-8}	2.7×10^{-8}	2.4×10^{-8}	2.3×10^{-8}
ATM 99-percentile differences	1.9×10^{-7}	2.0×10^{-7}	1.8×10^{-7}	1.9×10^{-7}	1.9×10^{-7}	1.9×10^{-7}
ATM Maximal absolute differences	1.1×10^{-3}	1.1×10^{-3}	1.1×10^{-3}	1.1×10^{-3}	1.1×10^{-3}	1.1×10^{-3}
OTM Average absolute differences	3.0×10^{-8}	3.9×10^{-8}	3.2×10^{-8}	3.2×10^{-8}	2.9×10^{-8}	2.0×10^{-8}
OTM 99-percentile differences	2.5×10^{-7}	2.6×10^{-7}	2.3×10^{-7}	2.4×10^{-7}	2.4×10^{-7}	2.5×10^{-7}
OTM Maximal absolute differences	1.5×10^{-3}	1.5×10^{-3}	1.5×10^{-3}	1.0×10^{-3}	1.0×10^{-3}	1.0×10^{-3}

^a792,000 distinct parameter sets for each trial. The first experiment deals with in-the-money call option (ITM, money-ness 90%), second with at-the-money call (ATM) and the final one is with respect to out-of-the-money call option (OTM, moneyness 110%).

Computation using upper limit $u = 1000$ is considered as the reference price.

The main advantage of this approach lies in its tractability. In fact, only the aforementioned Fourier integral has to be dealt with by numerical procedures. Moreover, its integrand is well behaved for a wide range of model parameters (see Table 1 and Figure 1).

For numerical evaluation, one also might set a finite upper integration limit u in the integral (or apply a suitable transformation). In case of the Heston model, it has been shown that when using the alternative option pricing formula as in Gatheral (2006), even a basic choice of the upper limit, $u = 100$, can be justified. For the presented long memory model, an illustration of the price sensitivity with respect to finite values of the integration bounds is provided by Figure 1 and by Table 1. In the latter, we display average, 99% quantile and maximal absolute differences between the reference price and convenient choices of the upper limits across various model parameter sets.

The choice of the upper integration limit plays a crucial role in the task of market calibration, especially when using heuristic optimization procedures. Since all values in

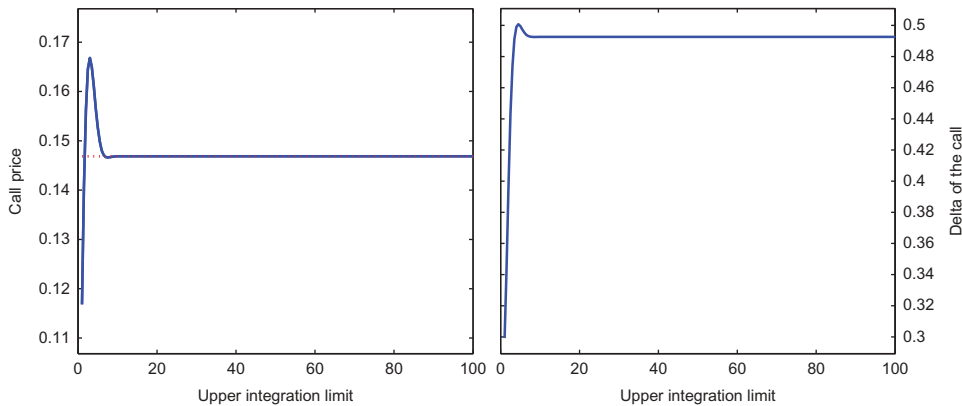


Figure 1. Numerical prices of a European call option and values of option δ using (19) with finite upper integration limits. Values correspond to the parameters of the contract: $S_0 = 1$, $K = 0.9$, $T = 1$, $r = 0.009$, model parameters $\kappa = 2$, $v_0 = 0.15$, $\bar{v} = 0.15$, $\xi = 0.5$, $\rho = -0.7$, $\lambda_j = 1$, $a_j = -0.5$, $\gamma_j = 1$, $H = 0.7$. The computation is performed with approximating factor $\varepsilon = 10^{-5}$.

the previous experiment provided a sufficient level of precision, we focus on computational efficiency when choosing integration bounds.

3. Market calibration

In this section, we employ the previously derived formula to retrieve risk-neutral market parameters with respect to a given set of traded call options. This procedure is known as a market calibration. Another way of looking at the task can be obtained via mathematical programming. One tries to find a set of model parameters Θ^* such that the criterion (40) is minimized.⁴

$$G(\Theta) = \sum_{i=1}^N w_i |C(S_0, K_i, T_i, r) - C^{\text{model}}(S_0, K_i, T_i, r, \Theta)|^p; \quad (40)$$

$$\Theta^* = \arg \inf_{\Theta \in A} G(\Theta), \quad (41)$$

for a market that consists of N traded call contracts. We set the value of $p, p \geq 1$, and we choose appropriate weight sequence $(w_i)_{i=1, \dots, N}$. An intuitive setting, $w_i = 1/N$ for all $i = 1, \dots, N$ and $p = 2$, brings us to the classic least square minimization problem. Using distinct weights for each contract, we can emphasize more liquid options over the less traded contracts. For the first empirical study, we calibrate models using three choices of weights which are defined,

$$w_i^{(1)} = \frac{1}{|C_i^{(\text{ask})} - C_i^{(\text{bid})}|}, \quad (42)$$

$$w_i^{(2)} = \frac{1}{\sqrt{|C_i^{(\text{ask})} - C_i^{(\text{bid})}|}}, \quad (43)$$

$$w_i^{(3)} = \frac{1}{(C_i^{(\text{ask})} - C_i^{(\text{bid})})^2}, \quad (44)$$

for $i = 1, \dots, N$. $C_i^{(\text{bid})}$, $C_i^{(\text{ask})}$ stand for a bid price of the i th market option and ask price, respectively. Also, we assume that the price spread is strictly positive for all quoted contracts. The minimization is with respect to simple bounds (see Table 2) which are introduced to ensure that all parameters stay in their domains (e.g. we consider $H \in [0.5, 1)$).

As several authors pointed out (e.g. Mikhailov and Nögel 2003), the minimization problem (41) is typically non-convex and without a very good initial guess, it might be hard to solve using local optimization techniques only. Hence, for the task of model comparison, we utilize global procedures, a genetic algorithm (GA) and simulated annealing (SA), as well as a local trust-region method for least square problems (LSQ).

Table 2. Parameter bounds for optimization problem.

	κ	v_0	\bar{v}	ξ	ρ	λ_j	a_j	γ_j	H
Lower bound	0	0	0	0	-1	0	-10	0	0.5
Upper bound	50	1	1	4	1	100	5	4	0.9999

Table 3. Optimizer settings for market calibration.

	GA criterion	Value	SA criterion	Value
<i>Evolution rules</i>				
	Population size	60	Annealing fun	Uniform direction, temp. step length
	Elite count	20%	Initial temperature	100
	Selection distribution	Uniform	Temperature fun	Exponential
	Mutation distribution	Gaussian	Reannealing interval	100
	Crossover fun	Random binary scatter	Acceptance fun	Exp. decay ^a
<i>Stopping rules</i>				
	No of generations	500	Maximum iterations	–
	Time limit	–	Time limit	–
	Fitness limit	–	Fitness limit	–
	Stall generations	60	Maximum fun. evaluations	100,000
	Fun. tolerance	1e – 8	Fun. tolerance	1e – 8
	Constraint tolerance	1e – 6		
	Stall time limit	–		
	Stall test	Average change		

^aExponentially decaying acceptance function (acceptancesa) is defined in Matlab documentation, see also www.mathworks.com/help/gads/simulated-annealing-options.html.

Results obtained by a global heuristic optimizer may vary significantly depending on how the routine is set. Most important criteria with respect to the global optimization are of two types: evolution and stopping rules. For both GA and SA, we altered stopping rule defaults used in the Matlab's Global Optimization Toolbox. First and foremost, we did not want the solver to stop prematurely – algorithms should terminate on a Function tolerance criterion, i.e. if the value of utility function (40) declines over the successive iteration by less than a given tolerance (1e – 8). For comparison purposes, we also employed the same settings for both less complex Heston model and LSV approach. The complete evolution and stopping rules used in the upcoming experiments are listed in Table 3.

3.1. Error measures

In order to compare the presented long memory volatility approach with the Heston model, we evaluate these market fit criteria,

$$\text{AAE}(\Theta) = \frac{1}{N} \sum_{i=1}^N |C_i - C_i^{\text{model}}(\Theta)|; \quad (45)$$

$$\text{AARE}(\Theta) = \frac{1}{N} \sum_{i=1}^N \frac{|C_i - C_i^{\text{model}}(\Theta)|}{C_i}; \quad (46)$$

$$\text{MAE}(\Theta) = \max_{i=1,2,\dots,N} |C_i - C_i^{\text{model}}(\Theta)|. \quad (47)$$

Due to varying price levels, the most interesting error measure is represented by AARE(Θ) which reflects the average absolute values of relative errors. ARE(Θ), on the other hand, represents the average absolute errors. We also might want to fit the calibrated surface with a preset error bound. The minimal bound that will suffice for each calibration trial is denoted by the maximal absolute error measure, MAE(Θ).

3.2. Empirical study – FTSE 100 vanilla call market

The main data set was obtained on 8 January 2014 and consists of 82 traded call options. The underlying is FTSE 100 index, quoted at 6721.80 points. The considered prices range from 17.5 to 514.5 and the data sample includes both in-the-money (ITM), at-the-money (ATM) and out-of-the-money (OTM) calls.⁵

Using combined optimization approaches that first utilize global (heuristic) methods and then the solution is improved by a local search method, we were able to retrieve superior results for both models. For these routines, the LSV model achieved a better market fit compared to the Heston model. The lowest value of the absolute relative error was obtained for the LSV model using a GA combined with a trust region method alongside weights $w^{(3)}$. However, the results for weights $w^{(1)}$, $w^{(2)}$ and also for a combined SA (SA + LSQ) are almost indifferent with respect to the selected error measures.

Option premia surface, created by the Heston model with calibrated parameters, is not consistent with market prices especially for OTM calls. This is partly because of the preset weights and partly, it might be caused by a low degree of freedom of the model.

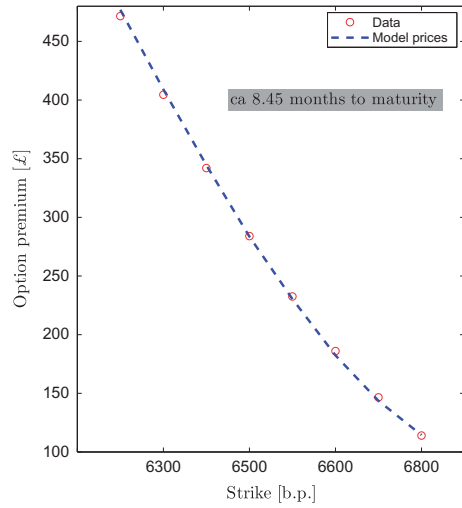
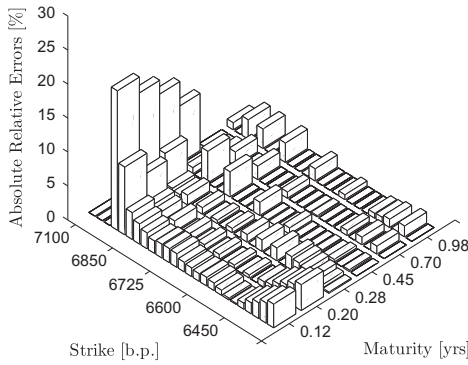
When calibrating the LSV model by using combined approaches, we retrieved values of the Hurst parameter $H \in [0.5935, 0.6654]$. This result is in line with several statistical studies on long memory estimation for realized volatility time series (e.g. Breidt, Crato, and De Lima 1998) and implied values are only slightly lower than their time-series estimates (Sobotka 2014, FTSE 100 realized volatilities, 2004–2014). All calibration errors are displayed in Table 4 and the corresponding price surfaces are depicted in Figure 2 for a combined GA and in Figure 3 for a combined SA method, respectively. We also illustrate errors retrieved only by heuristic optimization methods in Figure 4. Unlike previous calibration trials, the quality of market fit for the latter calibration is far from perfect.

3.3. Empirical study – stability of parameters in time – AAPL call options

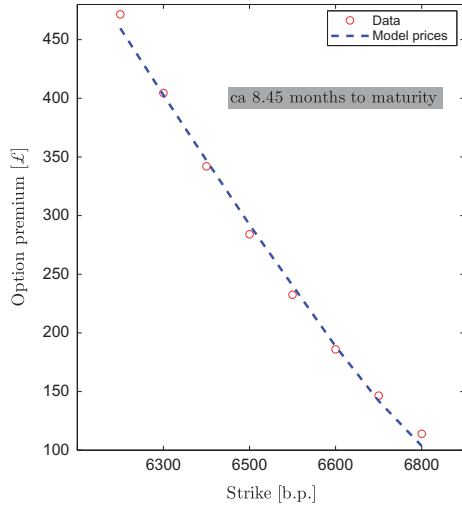
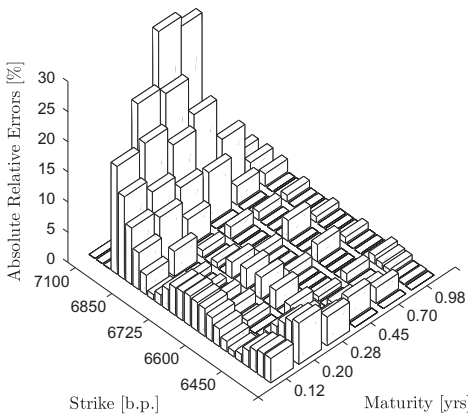
We also compared the models on Apple Inc. European call options traded on NYSE MKT LLC. This time, however, we considered 21 data sets, i.e. close quotes from Apple Inc. option market for all trading days in April 2015. Each data set included at least 113

Table 4. Calibration errors for weights $w^{(1)}$, $w^{(2)}$ and $w^{(3)}$.

Weights	Model	Error measure	GA	GA + LSQ	SA	SA + LSQ
$w^{(1)}$	LSV model	AARE (%)	4.29	2.34	3.79	2.34
		AAE ()	7.33	3.27	5.52	3.27
		MAE ()	49.34	17.13	24.17	17.13
	Heston model	AARE (%)	3.72	3.36	3.67	4.43
		AAE ()	6.54	5.85	7.83	6.22
		MAE ()	30.65	30.69	32.25	29.30
$w^{(2)}$	LSV model	AARE (%)	4.61	2.34	3.01	2.34
		AAE ()	7.57	3.27	5.04	3.27
		MAE ()	35.74	17.13	25.84	17.13
	Heston model	AARE (%)	3.10	3.35	3.78	3.52
		AAE ()	6.05	5.85	6.68	5.90
		MAE ()	30.84	30.69	31.09	30.68
$w^{(3)}$	LSV model	AARE (%)	5.95	2.33	4.33	2.34
		AAE ()	12.34	3.27	9.02	3.27
		MAE ()	81.79	17.14	45.71	17.13
	Heston model	AARE (%)	5.56	5.07	6.59	4.15
		AAE ()	7.16	6.42	9.89	8.20
		MAE ()	31.07	30.83	32.49	32.30



(a) Long memory SV model

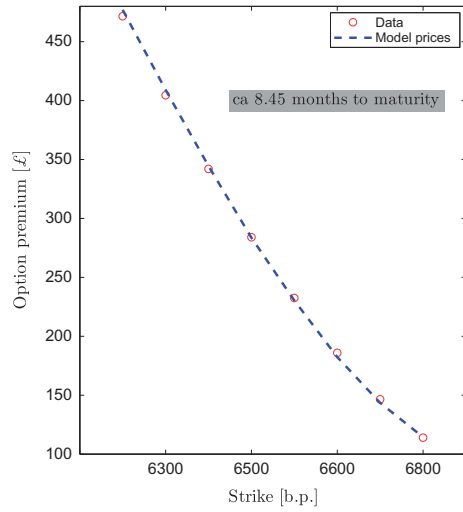
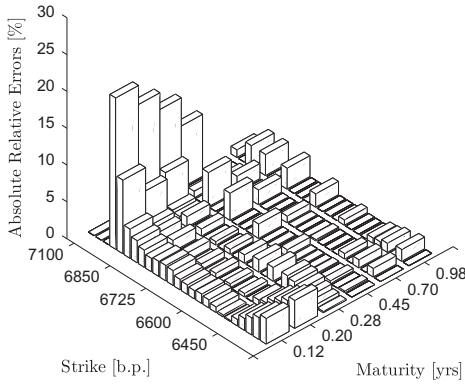


(b) Heston model

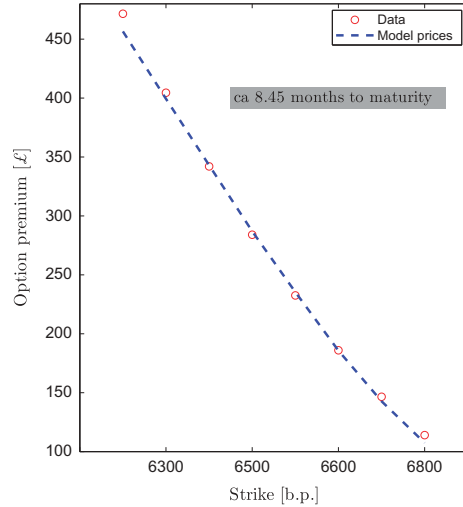
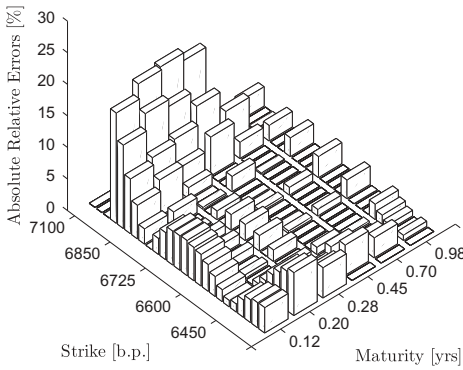
Figure 2. Calibration from FTSE 100 call option market using genetic algorithm combined with a local search method. Displayed average relative errors were obtained for weights $w_i^{(3)}$.

options (at most 212) and as in our previous experiment, we considered ITM, ATM and OTM contracts with moneyness ranging from 64.18% to 250.30% (in 30 April).⁶

Following results from previous study, we calibrated models using only GA + LSQ optimizers alongside weights $w^{(3)}$. As a main measure for model comparison, we considered weighted square errors. Namely, we compared both approaches with respect to the value of utility function $G(\Theta^*)$ (40) where Θ^* denotes the calibrated parameter set for a specific model.⁷ Unlike in previous experiment, some data sets contained options with very low prices where both models were prone to big relative errors. Therefore, we utilized the weighted error measure rather than AARE. However, one should not compare values of



(a) Long memory SV model

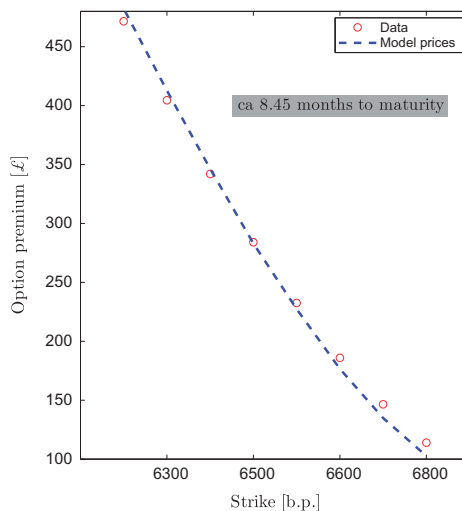
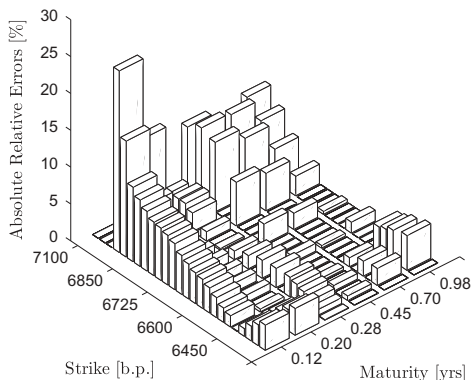


(b) Heston model

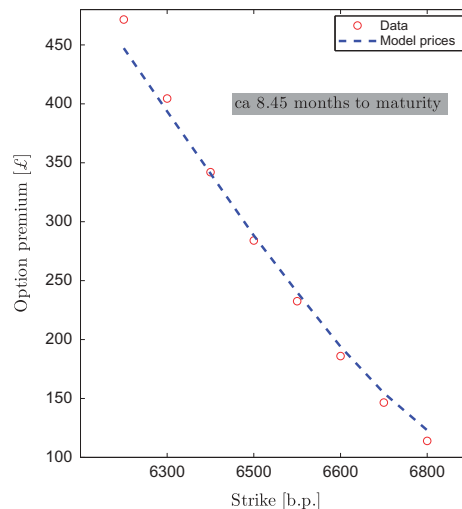
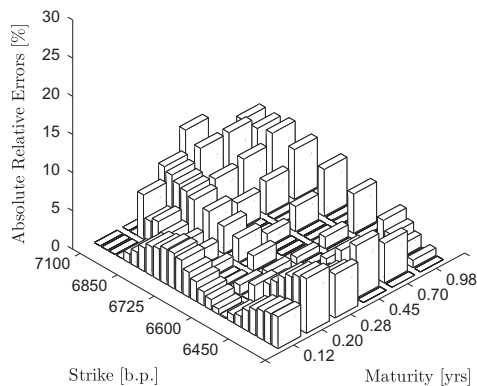
Figure 3. Calibration from FTSE 100 call option market using simulated annealing combined with a local search method. Displayed average relative errors were obtained for weights $w_i^{(1)}$.

$G(\Theta^*)$ across different trading days – the total number of options might vary for each data set. To measure stability of the calibrated parameters over time, we employed two criteria – average absolute difference and standard deviation of parameter values.

Obtained values $G(\Theta^*)$ ranged from 223.85 to 1711.37 and 346.61 to 1718.20 for LSV and Heston model, respectively. For 20 out of 21 data sets, Heston model was outperformed with respect to the weighted criteria – only on 29 April, we did not obtain a superior fit by LSV approach with our settings (479.51 vs. 528.85, parameters in Table 5). The lowest average absolute error (2.78%) was retrieved by LSV model on a data set from 4 April (Heston AARE – 3.37%, parameters in Table 5) and conversely,



(a) Long memory SV model



(b) Heston model

Figure 4. Calibration from FTSE 100 call option market using simulated annealing. Displayed average relative errors were obtained for weights $w_i^{(2)}$.

the worst value thereof was reached by Heston model on 20 April (5.77%). All results are conveniently listed in [Table 6](#).

Average absolute differences alongside standard deviations of calibrated parameters are shown in [Table 7](#). In our experiment, we managed to get similar values of the aforementioned measures for both models with respect to diffusion parameters. Evolution of ν_0 and $\bar{\nu}$ over time is depicted by [Figure 5](#). Calibration of LSV jump parameters, especially α_j and γ_j , provided us with more varying values compared to both diffusion parameters and the Hurst exponent. This might be due to the calibration procedure (global heuristic GA) and due to the fact that one can retrieve similar skew of

Table 5. Calibrated parameters for two trading days.

Date	κ	v_0	\bar{v}	ξ	ρ	λ_j	a_j	γ_j	H
LSV model									
10 April 2015	42.5642	0.1804	0.0598	3.8964	-0.1343	0.0088	0.2545	0.1922	0.5130
29 April 2015	17.3866	0.0496	0.0611	4.0000	0.0111	0.0058	-1.0000	4.0000	0.5000
Heston model									
10 April 2015	49.9995	0.1829	0.0632	2.3976	-0.0602				
29 April 2015	20.8354	0.0569	0.0688	2.5694	-0.1425				

Table 6. Calibration errors for weights $w^{(3)}$, Apple Inc. stock options.

Date	LSV model				Heston model			
	$G(\Theta^*)$	AARE (%)	AAE (\$)	MAE (\$)	$G(\Theta^*)$	AARE (%)	AAE (\$)	MAE (\$)
1 April 2015	223.85	4.16	0.32	1.42	346.61	5.49	0.34	1.50
2 April 2015	954.71	5.49	0.28	2.19	1368.39	4.58	0.26	1.77
6 April 2015	441.27	3.01	0.31	2.56	546.32	4.05	0.31	2.15
7 April 2015	501.13	3.42	0.31	1.28	665.78	4.33	0.35	1.81
8 April 2015	285.26	3.77	0.24	1.26	355.21	4.42	0.26	1.30
9 April 2015	697.95	3.67	0.37	1.58	715.79	4.07	0.37	1.55
10 April 2015	313.85	2.78	0.24	1.97	421.97	3.37	0.23	1.52
13 April 2015	588.05	3.15	0.24	1.25	704.98	3.31	0.26	1.27
14 April 2015	329.33	3.70	0.19	1.06	423.08	3.91	0.22	1.05
15 April 2015	408.80	3.44	0.27	1.72	542.65	3.80	0.25	1.29
16 April 2015	363.29	3.83	0.22	1.25	464.46	4.20	0.23	1.35
17 April 2015	453.36	3.06	0.20	1.14	544.60	3.20	0.21	1.08
20 April 2015	844.47	5.40	0.25	1.97	931.10	5.77	0.27	1.62
21 April 2015	686.47	5.46	0.22	1.80	856.57	4.32	0.25	1.50
22 April 2015	1711.37	5.03	0.42	3.15	1718.20	5.13	0.38	2.12
23 April 2015	693.37	3.97	0.24	1.22	700.66	3.83	0.22	1.15
24 April 2015	998.50	3.19	0.23	1.56	1062.61	3.21	0.22	1.37
27 April 2015	306.37	3.32	0.30	2.07	484.13	2.96	0.28	1.43
28 April 2015	1043.10	4.25	0.34	3.15	1093.86	3.76	0.35	3.60
29 April 2015	528.85	5.25	0.29	2.27	479.51	3.91	0.29	2.63
30 April 2015	517.68	3.92	0.20	1.33	527.31	3.88	0.20	1.28

Table 7. Stability of calibrated parameters.

Model	Measure	κ	v_0	\bar{v}	ξ	ρ	λ_j	a_j	γ_j	H
LSV	Average abs. difference	5.671	0.024	0.003	0.963	0.232	0.006	1.017	1.434	0.0596
	Standard deviation	11.110	0.049	0.003	0.976	0.294	0.006	1.331	1.459	0.084
Heston	Average abs. difference	8.744	0.0344	0.003	0.921	0.142				
	Standard deviation	10.702	0.052	0.003	0.957	0.188				

the volatility smile for different combinations of jump parameters. This shortfall can be partially improved by incorporating penalizing term in the utility function $G(\Theta)$ or by using local-search algorithm only (e.g. with initial guess from previous day calibration).

4. Summary

In the first part of the article, an alternative formula for pricing European options under a LSV model was derived. The formula is in a semi-closed form – one has to numerically evaluate a Fourier transform integral (19). For most of the observed market parameters, truncation of the upper integral bound alongside an appropriate numerical procedure leads to satisfactory results both in terms of precision (see Figure 1 and Table 1) and computational efficiency.⁸

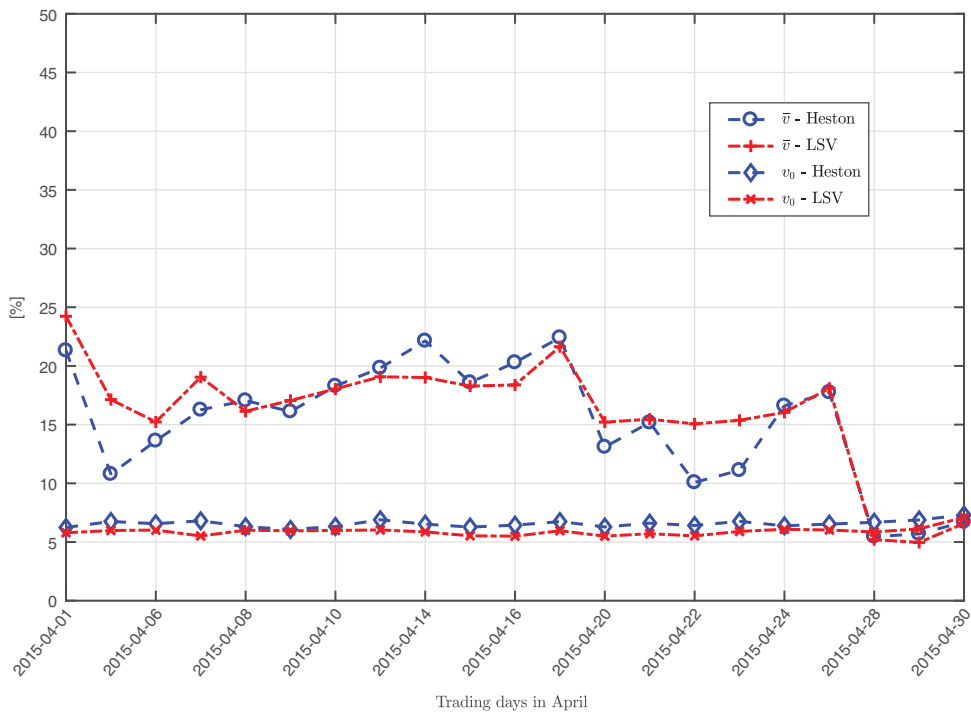


Figure 5. Evolution of calibrated parameters v_0 , \bar{v} for both models.

In practice, one is typically interested in a real-data performance of a particular model. To illustrate the quality of market fit, we introduced two empirical studies, both of them included a comparison with a popular approach, the Heston model. In the first study, we utilized traded European call options on FTSE 100 index. Also, four different optimization routines and three sets of calibration weights were applied. Heuristic algorithms provided a solution that was suboptimal but (especially in case of GA) the solution represented a good initial guess for a local-search method. Since the optimization problem is non-convex, local routines, as the trust region or Levenberg–Marquardt method, need to be initialized in the vicinity of a (global) minimum.

The second study involved 21 data sets, i.e. Apple Inc. call options for all trading days in April 2015. This time, we applied GA and refined the solution by LSQ. On 20 days, LSV approach outperformed Heston model having superior (weighted) residual sum of squares as highlighted in Table 6. The inferior result on the data set from 29 April (parameters in Table 5) was obtained after GA procedure provided initial guess that for three parameters reached parameter bounds. The solution can be improved by providing better initial guess (preferably not very close to parameter bounds) or by increasing bounds. We increased an upper bound for ξ to 10 for both models,⁹ Heston solution for 29 April remained the same, unlike under LSV where parameters changed to:

κ	v_0	\bar{v}	ξ	ρ	λ_j	a_j	γ_j	H
18.3005	0.0544	0.0649	8.3030	-0.0753	0.0046	-1.0010	0.1477	0.5000

which provided $G(\Theta) = 473.61$ and 4.15% AARE.

We managed to calibrate the LSV model using combined optimization approaches mostly with better error measures compared to the Heston model. This result was expected, since the proposed model utilizes more parameters and thus has more degrees of freedom to fit the market. However, this might not be the case of all stochastic volatility models as was shown by Duffie, Pan and Singleton (2000). The authors compare market fits of diffusion models with jumps in the underlying only to results obtained by models with jumps both in the underlying and volatility process. Although the latter approaches typically include more parameters, they might not provide a better market fit of observed option prices.

The proposed LSV model might provide better market fit compared to Heston model; however, an increased complexity of the calibration problem is the price one has to pay. To improve this issue, one might derive a pricing formula using the complex Fourier transform as suggested by Lewis (2000) for Heston model. Since calibrated parameters do change over time, one might also be interested in a time-dependent version of the LSV approach, either with piece-wise constant (Mikhailov and Nögel 2003) or functional parameters (Osajima 2007).

Another important aspect, which is out of scope of this paper, would be a comparison of the empirical and model distribution for the underlying. We commented on realized volatility time-series estimates of H which are only slightly greater than implied values obtained by calibration of the LSV approach (w.r.t. FTSE 100 index).

Notes

1. A risk-neutral probability measure for this model is not uniquely defined due to the incompleteness of the market, purely for derivatives pricing we do not need to specify it. Comments on the equivalent martingale measures for classical stochastic volatility models are available, for instance, in Sircar and Papanicolaou (1999) and references therein.
2. This assumption is taken into consideration in many jump-diffusion stock models, e.g. Bates (1996).
3. This is possible due to the stochastic independence with diffusion processes and log-normal distribution of the jumps, see Gatheral (2006).
4. In case of the presented approach, Θ^* takes form: $\Theta^* := \left\{ \kappa^*, v_0^*, \bar{v}^*, \xi^*, \rho^*, \lambda_j^*, \alpha_j^*, \gamma_j^*, H^* \right\}$
5. Data set obtained from OMON Screen, Bloomberg L.P. 2014.
6. Other data sets possessed slightly narrower moneyness range.
7. In fact, $G(\Theta^*)$ represents weighted least squares of the market fit.
8. One can calibrate the model using heuristic algorithms that evaluate model prices very frequently.
9. Under Heston model, ξ represents volatility of volatility and thus, one would intuitively expect that the increased upper bound would not affect the solution. Under the LSV approach, however, vol. of vol. takes the following form, $\xi \varepsilon^{H-1/2}$ and thus, ξ might take greater values.

Acknowledgements

This work was supported by the GACR Grant 14-11559S Analysis of Fractional Stochastic Volatility Models and their Grid Implementation. Computational resources were provided by the CESNET LM2015042 and the CERIT Scientific Cloud LM2015085, provided under the programme “Projects of Large Research, Development, and Innovations Infrastructures”.

Disclosure statement

No potential conflict of interest was reported by the authors.

Funding

This work was supported by the GACR Grant 14-11559S Analysis of Fractional Stochastic Volatility Models and their Grid Implementation.

References

- Asai, M., M. McAleer, and M. C. Medeiros. 2012. "Modelling and Forecasting Noisy Realized Volatility." *Computation Statist Data Analysis* 56 (1): 217–230. doi:10.1016/j.csda.2011.06.024.
- Bates, D. S. 1996. "Jumps and Stochastic Volatility: Exchange Rate Processes Implicit in Deutsche Mark Options." *Review of Financial Studies* 9 (1): 69–107. doi:10.1093/rfs/9.1.69.
- Beran, J., Y. Feng, S. Ghosh, and R. Kulik. 2013. *Long-Memory Processes*. Heidelberg: Springer, Probabilistic properties and statistical methods.
- Bollerslev, T., and O. H. Mikkelsen. 1996. "Modeling and Pricing Long Memory in Stock Market Volatility." *Journal of Econometrics* 73 (1): 151–184. doi:10.1016/0304-4076(95)01736-4.
- Breidt, F. J., N. Crato, and P. De Lima. 1998. "The Detection and Estimation of Long Memory in Stochastic Volatility." *Journal of Econometrics* 83 (1–2): 325–348. doi:10.1016/S0304-4076(97)00072-9.
- Čekal, M., 2012 The Effect of Long Memory Volatility on Option Pricing. Master's thesis, University of Amsterdam.
- Comte, F., L. Coutin, and E. M. Renault. 2012. "Affine Fractional Stochastic Volatility Models." *Annals of Finance* 8 (2–3): 337–378. doi:10.1007/s10436-010-0165-3.
- Comte, F., and E. Renault. 1998. "Long Memory in Continuous-Time Stochastic Volatility Models." *Mathematical Finance* 8 (4): 291–323. doi:10.1111/mafi.1998.8.issue-4.
- Cont, R. 2001. "Empirical Properties of Asset Returns: Stylized Facts and Statistical Issues." *Quantitative Finance* 1 (2): 223–236. doi:10.1080/713665670.
- Ding, Z., C. W. J. Granger, and R. F. Engle. 1993. "A Long Memory Property of Stock Market Returns and A New Model." *Journal of Empirical Finance* 1 (1): 83–106. doi:10.1016/0927-5398(93)90006-D.
- Duffie, D., J. Pan, and K. Singleton. 2000. "Transform Analysis and Asset Pricing for Affine Jump-Diffusions." *Econometrica* 68: 1343–1376. doi:10.1111/ecta.2000.68.issue-6.
- Gatheral, J. 2006. *The Volatility Surface: A Practitioner's Guide*. Hoboken, NJ: Wiley Finance (John Wiley & Sons).
- Granger, C. W. J., and R. Joyeux. 1980. "An Introduction to Long-Memory Time Series Models and Fractional Differencing." *Journal of Time Series Analysis* 1 (1): 15–29. doi:10.1111/j.1467-9892.1980.tb00297.x.
- Heston, S. L. 1993. "A Closed-Form Solution for Options with Stochastic Volatility with Applications to Bond and Currency Options." *Review of Financial Studies* 6: 327–343. doi:10.1093/rfs/6.2.327.
- Intarasit, A., and P. Sattayatham. 2011. "An Approximate Formula of European Option for Fractional Stochastic Volatility Jump-Diffusion Model." *Journal of Mathematics and Statistics* 7 (3): 230–238. doi:10.3844/jmssp.2011.230.238.
- Koopman, S. J., B. Jungbacker, and E. Hol. 2005. "Forecasting Daily Variability of the S&P 100 Stock Index Using Historical, Realised and Implied Volatility Measurements." *Journal of Empirical Finance* 12 (3): 445–475. doi:10.1016/j.jempfin.2004.04.009.
- Lewis, A. L. 2000. *Option Valuation under Stochastic Volatility, with Mathematica Code*. Newport Beach, CA: Finance Press.
- Mandelbrot, B., and J. Van Ness. 1968. "Fractional Brownian Motions, Fractional Noises and Applications." *SIAM Review* 10: 422–437. doi:10.1137/1010093.

- Martens, M., D. Van Dijk, and M. De Pooter, Modeling and Forecasting S&P 500 Volatility: Long Memory, Structural Breaks and Nonlinearity. (2004), Technical report TI 04-067/4, Tinbergen Institute.
- Mikhailov, S., and U. Nögel (2003) Heston's Stochastic Volatility Model-Implementation, Calibration and Some Extensions., Wilmott magazine, pp. 74-79.
- Øksendal, B. (2003) *Stochastic Differential Equations. An Introduction With Applications*. Sixth edition. Universitext. Springer-Verlag, Berlin. ISBN: 3-540-04758-1
- Osajima, Y., The Asymptotic Expansion Formula of Implied Volatility for Dynamic SABR Model and FX Hybrid Model. (2007), Technical report, BNP Paribas Available from SSRN: <http://ssrn.com/abstract=965265>.
- Shreve, S. E. 2004. *Stochastic Calculus for Finance. II*. New York: Springer Finance Springer-Verlag.
- Sircar, K. R., and G. C. Papanicolaou. 1999. "Stochastic Volatility, Smile & Asymptotics." *Applied Mathematical Finance* 6 (2): 107-145. doi:10.1080/135048699334573.
- Sobotka, T., 2014 Stochastic and fractional stochastic volatility models. Master's thesis, University of West Bohemia.
- Taylor, S. 1986. *Modelling Financial Time Series*. Chichester: John Wiley & Sons.
- Thao, T. H. 2006. "An Approximate Approach to Fractional Analysis for Finance." *Nonlinear Analysis: Real World Applications* 7: 124-132. doi:10.1016/j.nonrwa.2004.08.012.
- Thao, T. H., and T. T. Nguyen. 2003. "Fractal Langevin Equation." *Vietnam Journal Mathematics* 30 (1): 89-96.
- Zähle, M. (1998). Integration With Respect To Fractal Functions And Stochastic Calculus. I. *Probability Theory Related Fields* 111 (3): 333-374. doi:10.1007/s004400050171
- Zumbach, G. 2013. *Discrete Time Series, Processes, and Applications in Finance*. Heidelberg: Springer Finance (Springer).
- Zumbach, G., and L. Fern'Andez. 2013. "Fast and Realistic European ARCH Option Pricing and Hedging." *Quantitative Finance* 13 (5): 713-728. doi:10.1080/14697688.2012.750009.
- Zumbach, G., and L. Fern'Andez. 2014. "Option Pricing with Realistic ARCH Processes." *Quantitative Finance* 14 (1): 143-170. doi:10.1080/14697688.2013.816437.